Investigation of mechanical alloying of Ti–Al compounds using perturbed γγ-angular correlation spectroscopy, x-ray diffraction, and differential scanning calorimetry

St. Lauer, Z. Guan, H. Wolf, and Th. Wichert
Technische Physik, Universität des Saarlandes, D-66041 Saarbrücken, Germany

(Received 21 January 2002; accepted 3 June 2002)

$Ti_{0.50}Al_{0.50}$ and $Ti_{0.75}Al_{0.25}$ compounds were mechanically alloyed by ball milling of elemental Ti and Al powders. Radioactive ^{111}In atoms incorporated into these compounds were used to investigate the different locally ordered crystalline structures by perturbed γγ-angular correlation spectroscopy (PAC). The formation of the intermetallic compounds γ–TiAl and α_2–Ti_3Al was observed on an atomic scale and occurred as a consequence of the heat treatment of mechanically alloyed $Ti_{0.50}Al_{0.50}$ and $Ti_{0.75}Al_{0.25}$, respectively. Due to the sensitivity of PAC to local order on an atomic scale, information about formation conditions and thermal stability of a new metastable phase with an ordered tetragonal crystal structure is presented for $Ti_{0.50}Al_{0.50}$ samples. In addition, the formation of the ordered phase Ti_2AlN was observed, indicating the incorporation of N during the milling process. The PAC investigations were complemented by x-ray diffraction and differential scanning calorimetry measurements.

I. INTRODUCTION

Intermetallic compounds of Ti and Al are of technological interest for high-temperature applications.[1] These materials are characterized by a low density, high melting point, and good resistance against oxidation. Until now, the widespread use of Ti-aluminides, however, is hampered as well by the poor ductility and fracture toughness at low temperatures as by the poor strength at high temperatures. To improve these deficiencies, attempts are made with respect to the control of the microstructure, such as grain refinement, and of the precipitation of a second phase, such as a nitride, carbide, or oxide phase. Thus, the precipitation of Ti_2AlN in γ–TiAl leads to an improved strength up to temperatures of about 1300 K.[2]

Especially, the process of mechanical alloying by ball milling offers advantages for the production of Ti–Al compounds and, therefore, has been investigated in detail.[3] Ball milling leads to a small grain size, thereby improving the mechanical properties,[4] and the produced powders are suitable for powder metallurgical preparation methods, such as net shaping. In contrast to ingot metallurgy, it is possible to produce nonequilibrium phases by mechanical alloying, such as amorphous phases or supersaturated solid solutions. The addition of a reactive medium during the milling process modifies the powders chemically. Thus, the addition of gaseous N or liquid heptane to the Ti and Al powders was attempted to increase the hardness through the precipitation of Ti_2AlN[5] and $Ti_4Al_2C_2$,[6] respectively. However so far experimental techniques that provide local information and are sensitive to local order on an atomic scale have not been employed to these problems in a systematic way. As a consequence, it has been difficult if not impossible at all to distinguish between phases with different local structure or to detect the presence of local defects in otherwise long-range-ordered crystalline phases.

The experimental data presented here were obtained by applying perturbed γγ-angular correlation spectroscopy (PAC) with radioactive ^{111}In atoms as local probes for the characterization of the mechanically alloyed Ti–Al compounds on an atomic scale. The characterization was performed by measuring the electric field gradient (EFG) at the site of the radioactive probe atom, whereby the EFG was typical for the local atomic structure about the probe atom and, therefore, provided information about the local environment of the probe atom on an atomic scale. It comprises the local symmetry and chemical order of neighboring atoms as well as the detection of structural point defects.[7] In this work, $Ti_{0.50}Al_{0.50}$ and $Ti_{0.75}Al_{0.25}$ compounds are studied in order to continue similar investigations of the Al-rich $Ti_{0.25}Al_{0.75}$ compounds.[8] Thus, the present paper describes the sequence of phase formation of mechanically alloyed Ti and Al powder blends during thermal annealing by PAC and the

extracted information is compared with that obtained by x-ray diffraction (XRD) and differential scanning calorimetry (DSC).

II. EXPERIMENTAL DETAILS

As mentioned above, PAC experiments yield information about the local environment of suitable radioactive probe atoms by measuring the local EFG. The probe atom ^{111}In decays to an excited state of its daughter isotope ^{111}Cd (Fig. 1), which emits two γ quanta and, thereby, populates a spin $I^{\pi} = 5/2^{+}$ nuclear level with a lifetime $\tau = 123$ ns. The spatial emission probability of the second γ quantum with respect to the direction of the first one shows anisotropy due to the conservation of angular momentum during the decay process. The EFG is the second derivative of the electrostatic potential and is described by its second rank traceless tensor V_{ij}, which in its principle axes system is completely described by its largest component V_{zz} and the asymmetry parameter $\eta = (V_{xx} - V_{yy})/V_{zz}$. The asymmetry parameter assumes the values $0 \leqslant \eta \leqslant 1$ if $|V_{xx}| \leqslant |V_{yy}| \leqslant |V_{zz}|$ is chosen. Since the strength of the EFG decreases with the distance r of a generating charge by r^{-3}, this parameter is particularly sensitive to the local environment about the probe atom. The EFG at the site of the probe nucleus is detected by the hyperfine interaction with the quadrupole moment Q of the $I^{\pi} = 5/2^{+}$ state of the daughter isotope ^{111}Cd, causing a threefold splitting of this nuclear level. In consequence, the emission probability of γ_2 with respect to γ_1 is modulated in time, and this modulation is governed by three frequencies ω_1, ω_2, and $\omega_3 = \omega_1 + \omega_2$, which are proportional to the product QV_{zz}. The strength of the EFG is usually expressed by the quadrupole coupling constant $\upsilon_Q = eQV_{zz}/h$ and the asymmetry parameter η is deduced from the ratio ω_2/ω_1. In a PAC experiment,

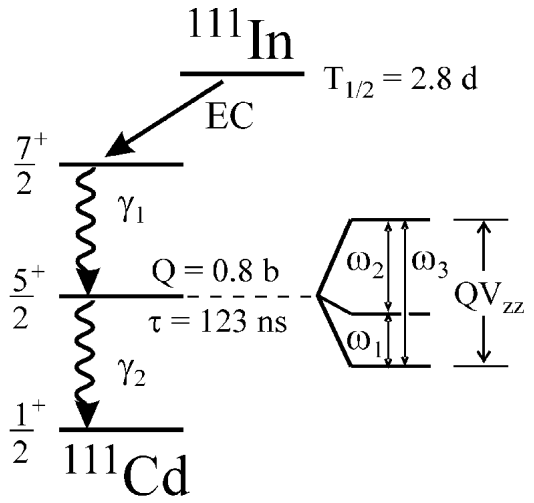

FIG. 1. Radioactive decay scheme of the PAC probe ^{111}In showing the electron capture decay (EC) to ^{111}Cd.

the number of γ_1–γ_2 coincidences as a function of the time passed between the emission of the first and the second γ quantum is recorded under fixed angles θ. In case of polycrystalline samples, the number of recorded coincidences is described by

$$N(\theta,t) = N_0 \cdot e^{-t/\tau} \cdot [1 + P_2(\cos\theta) \cdot R(t)] + B \quad . \quad (1)$$

Here, N_0 denotes the number of recorded coincidences at $t = 0$, B the time-independent background caused by chance $\gamma\gamma$ coincidences and $P_2(\cos\theta)$ is the second-order Legendre polynomial. The function of interest

$$R(t) = A_2 \cdot \left\{ f \cdot \left(s_0 + \sum_{n=1}^{3} s_n \cdot \cos\omega_n t \cdot e^{-\sigma_n t} \right) + (1 - f) \right\} \quad , \quad (2)$$

is extracted from the coincidence spectra $N(\theta,t)$ yielding the three frequencies ω_1, ω_2, and ω_3.[9] The amplitude f of the modulation corresponds to the fraction of probe atoms that reside in a crystalline phase or in a local environment producing the nonzero EFG and $(1 - f)$ denotes the fraction of probe atoms with zero EFG. The damping coefficients σ_n arise from an EFG distribution ΔV_{zz}, which can be caused by local lattice imperfections, impurities, or defects. In Eq. (2) and for the evaluation of the present experimental data, this distribution is assumed to be of Lorentzian shape and is characterized by $\Delta\upsilon_Q \sim \Delta V_{zz} \sim \sigma_n$. In the case of more than one single local environment characterized by a nonzero EFG, f is split into different fractions $f(i)$, whereby each fraction is characterized by its own frequency triplet $\omega_n(i)$. The EFG of a specific local structure behaves like a fingerprint and, therefore, can be used to identify such local structures in new materials. By using four γ-detectors, 12 coincidence spectra are recorded simultaneously. A more detailed description of PAC spectroscopy, applied to the investigations of metals, can be found elsewhere.[9,10] The absolute number of probe atoms needed for a PAC experiment is in the order of 10^{11} to 10^{12} atoms per sample corresponding to a concentration below 1 ppm. This concentration is below the concentration of residual impurities and does not alter the properties of the sample. Therefore, it is easily possible to compare the results of this technique with those obtained by other analytical techniques, such as XRD and DSC.

The XRD measurements were carried out at a Siemens D5000 θ-θ diffractometer (Germany) using a Mo anode. The investigated samples were treated identically to the samples used for the PAC experiments with the only exception that no radioactive ^{111}In was added. The grain size of nanocrystalline samples was determined from the

line shape of the diffraction peaks according to the method of Williamson and Hall.[11] When the results of PAC and XRD are compared, their specific sensitivities have to be taken into account. Because of its short-range sensitivity, PAC is sensitive to local structures, such as to the chemical order of an intermetallic compound about the probe atom. Such a local structure gives rise to a well-defined EFG also in the absence of a periodicity on a larger scale. On the other hand, a chemically disordered solid solution does not give rise to a well-defined EFG but rather to a distribution of EFG because of the large number of possible nonequivalent local environments about the probe atoms caused by the random occupation of the neighboring lattice sites. In contrast, XRD is mainly sensitive to the periodic arrangement of atoms on a larger scale but less to the local chemical disorder. However, the detection of chemical order becomes visible only by the appearance of additional superlattice lines. Since these lines have small intensities in case of incompletely ordered lattices, the chemical order may be difficult to detect.[12] In this respect, both experimental methods complement each other.

Thermodynamic properties of the samples were investigated by DSC using a Netzsch DSC 202 (Selb, Germany) setup. The investigated powders were heated at a rate of 20 K/min and cooled at a rate of 50 K/min in an Al_2O_3 crucible under continuous flow of purified Ar. To detect irreversible transformations of the metastable phases, produced by the ball milling process, into equilibrium phases, the baseline of the DSC plot was determined by subtracting the values of a second run, which was recorded immediately after the first one. The data obtained by DSC supply information about the temperatures of thermally induced phase transformations. When the results of DSC and PAC are compared, the different conditions of thermal treatment have to be taken into account. Whereas in the DSC experiment the temperature is continuously increased, in case of PAC and XRD, the heat treatment consists of an isochronal (16 h) annealing program at some distinct temperatures.

For mechanical alloying, powders of Ti (purity 99.98%) and of Al (99.99%) with particle sizes smaller than 150 μm were mixed and filled into hardened steel vials under Ar atmosphere. The powders were milled in a standard Spex 8000 ball-mill (Grasbrunn, Germany) for times ranging between 2 and 52 h. The powders were handled and milled in a glove-box under Ar atmosphere.

The ^{111}In probe atoms were incorporated into the milled powder samples by diffusion inside of an evacuated quartz ampoule (10^{-5} mbar) at a temperature of $T_{diff} = 690$ K for a time of 16 h. Subsequently, the samples were annealed at temperatures up to 1060 K without opening the quartz ampoule. Following each temperature step, a PAC spectrum was recorded at room temperature. Since the concentration of the In probe atoms is always below 1 ppm, the phase formation in the mechanically alloyed and annealed Ti–Al samples should not be affected by the In atoms.

III. RESULTS

A. $Ti_{0.50}Al_{0.50}$

Different samples consisting of 50 at.% Ti and 50 at.% Al were alloyed by ball-milling for $t_{mill} = 2$, 4, 8, 13, and 23 h (see Table I). After a milling time of 13 h (sample #A4), the XRD analysis does not show any diffraction peaks corresponding to elemental Ti or Al but reveals the formation of a solid solution with a hexagonal-close-packed (hcp) lattice structure. This result is in agreement with the data from the literature obtained under comparable experimental conditions,[12,13] indicating that the process of mechanical alloying is terminated and a homogeneous alloy is formed. The grain size was determined to about 20 nm on the basis of the analysis of the XRD data.

Following the characterization of the as-milled state by XRD, the ^{111}In probe atoms were diffused into this sample. The recorded PAC time spectrum R(t) as well as its Fourier transform F(ω) [Fig. 2(a), left and right panel, respectively] do not show any frequency triplet, which would correspond to a well-defined single EFG. Rather, a broad EFG distribution is visible, indicating that the local arrangement of neighboring atoms is different for each probe atom. This EFG distribution can belong either to probe atoms that did not diffuse into the crystallites and still reside at grain boundaries or to ^{111}In atoms incorporated at regular lattice sites of chemically disordered Ti–Al crystallites. Thus, in agreement with the XRD data, the observed EFG distribution can be explained by a random occupation of the hcp lattice sites about the ^{111}In probes by Ti and Al atoms in the Ti–Al solid solution.

After annealing at 880 K for 16 h, two different well-defined EFG are visible [Fig. 2(b)], and the observed fractions indicate that about 20% of the ^{111}In atoms are incorporated in the corresponding two different locally ordered structures. When the annealing temperature is increased to 1060 K, the EFG distribution completely

TABLE I. Mechanically alloyed Ti–Al powders investigated in this work.

Composition	Sample no.	Milling time (h)
$Ti_{0.50}Al_{0.50}$	A1	2
	A2	4
	A3	8
	A4	13
	A5	23
$Ti_{0.75}Al_{0.25}$	B1	16
	B2	52

disappears, and at the same time, the number of ^{111}In atoms located in both ordered structures increases significantly [Fig. 2(c)]. The analysis yields that 60% of the ^{111}In atoms exhibit an EFG characterized by $\upsilon_Q = 142$ MHz and $\eta = 0$, which is known to be caused by the intermetallic compound γ–TiAl.[14] Fan and Collins observed this EFG for the tetragonal Ll_0 structure of γ-TiAl, which is composed of alternating layers of Ti and Al atoms along the *c* axis [Fig. 3(a)]. Since only a single axially symmetric EFG ($\eta = 0$) was observed in their experiment, they concluded that ^{111}In is exclusively incorporated on the site of the isovalent Al atoms. In contrast, the second EFG ($f = 12\%$) characterized by $\upsilon_Q = 259$ MHz and $\eta = 0$ was not observed in Ti–Al compounds before. The XRD analysis of a second $Ti_{0.50}Al_{0.50}$ sample, treated identically to this sample (#A4), shows two ordered phases after annealing at 1060 K [Fig. 4(a)]: Firstly, the pattern of tetragonal γ–TiAl confirming the assignment of the first EFG to γ–TiAl and, secondly, a phase attributed to hexagonal Ti_2AlN with an $AlCCr_2$-type crystal structure. Therefore, the EFG characterized by $\upsilon_Q = 259$ MHz is assigned to ^{111}In atoms located in the ordered phase of Ti_2AlN. As will be discussed in context with $Ti_{0.75}Al_{0.25}$, this latter assignment corrects an earlier interpretation,[15] which assigned this EFG to α_2–Ti_3Al [Fig. 3(b) and see below]. The formation of Ti_2AlN clearly shows the contamination of the Ti–Al powder by N impurities.

For sample #A4, the evolution of the intermetallic phases was investigated by DSC [Fig. 5, top panel]. The DSC spectrum shows two sharp, exothermal peaks at 845 and 1000 K, respectively. By comparing the DSC results with the fraction of ^{111}In atoms that are incorporated in γ–TiAl ($f_{\gamma\text{–TiAl}}$) and in Ti_2AlN (f_{Ti_2AlN}) during isochronal annealing [Fig. 5, bottom panel], it is obvious that the DSC peak at 845 K coincides with the steepest increase

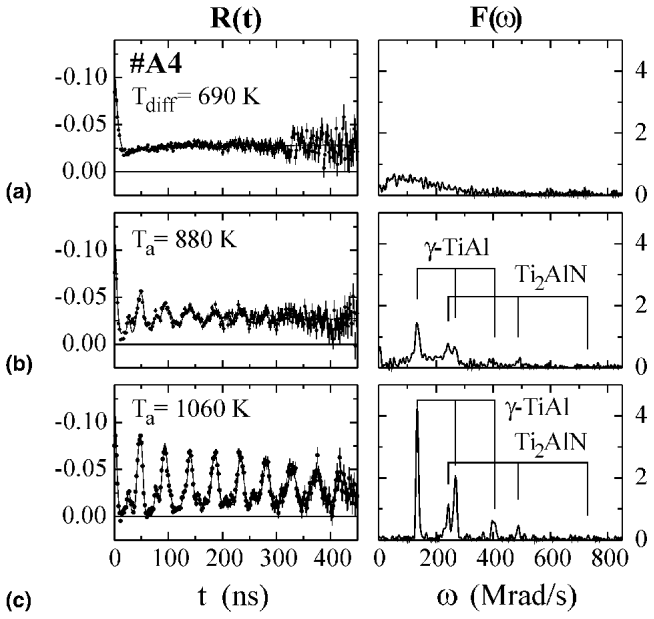

FIG. 2. PAC spectra of mechanically alloyed $Ti_{0.50}Al_{0.50}$ (sample #A4). The spectra were recorded after diffusion of ^{111}In at 690 K, and annealing at 880 and 1060 K. The phase γ–TiAl is characterized by $\upsilon_Q = 142$ MHz, $\eta = 0$, and Ti_2AlN by $\upsilon_Q = 259$ MHz, $\eta = 0$.

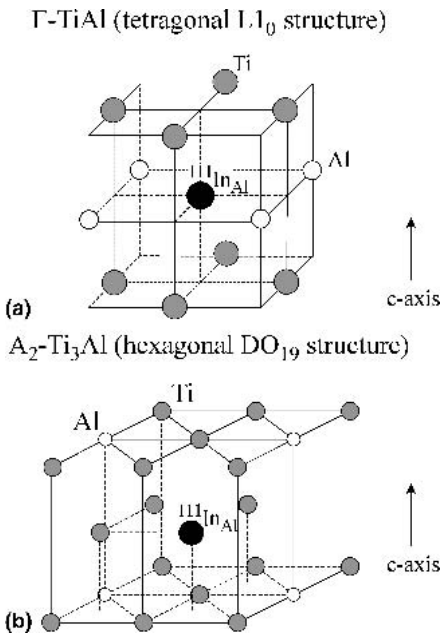

FIG. 3. Lattice structure of (a) γ–TiAl and (b) α_2–Ti_3Al. The ^{111}In probe atoms are assumed to occupy Al sites.

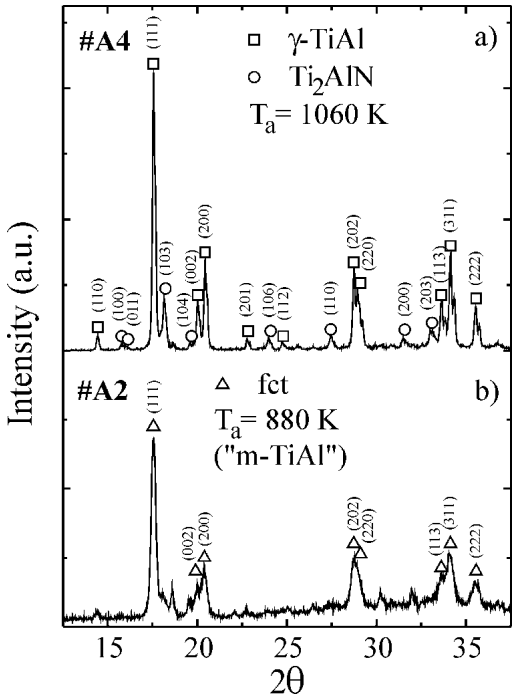

FIG. 4. XRD data of two $Ti_{0.50}Al_{0.50}$ samples: (a) recorded after milling for 13 h (sample #A4) and annealing at 1060 K, and (b) after milling for 4 h (sample #A2) and annealing at 880 K.

of f_{Ti_2AlN} and the peak at 1000 K with the steepest increase of $f_{\gamma\text{–TiAl}}$. Therefore, it is concluded that the DSC peak at 845 K corresponds to the ordering transition of Ti_2AlN and the peak at 1000 K to that of γ–TiAl.

In contrast to sample #A4 (t_{mill} = 13 h, see Table I), the XRD spectrum of sample #A2 (t_{mill} = 4 h), directly recorded after the milling process still exhibits the diffraction peaks of elemental Ti and Al. The mechanical alloying process is obviously not yet completed and the final phase formation, observable at 1060 K, requires the interdiffusion of Ti and Al atoms. The PAC data show an EFG distribution after diffusion of ^{111}In at 690 K [Fig. 6(a)]. After annealing the sample at 790 K, this distribution changes to a reduced width of $\Delta\nu_Q$ = 16 MHz centered at $\overline{\nu_Q}$ = 38 MHz [Fig. 6(b)]. Following annealing at 880 K, a new crystalline structure called m-TiAl is observed [Fig. 6(c)], which is characterized by a well-defined EFG (ν_Q = 57 MHz and η = 0.1). The EFG disappears after annealing at 1060 K [Fig. 6(d)] and the EFG of γ–TiAl, already observed in sample #4, is detected by 70% of the probe atoms. Since the temperature treatment at 1060 K leads to the disappearance of m-TiAl and the formation of γ–TiAl, it is concluded that m-TiAl corresponds to a metastable precursor, which developed during the interdiffusion of Ti and Al at the annealing temperature T_a = 880 K. The heat treatment at 1060 K, finally, effects the formation of the equilibrium phase γ–TiAl.

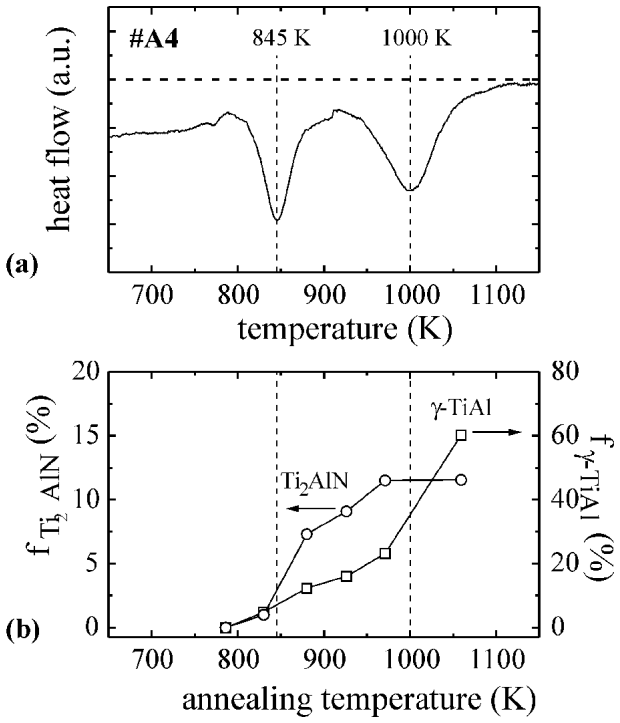

FIG. 5. For sample #A4, comparison of (a) DSC results and (b) the fraction of ^{111}In atoms observed by PAC in γ–TiAl and Ti_2AlN.

The crystal structure of m-TiAl was studied using the XRD data of sample #A2 after annealing at 880 K [Fig. 4(b)]. The XRD spectrum mainly shows a face-centered tetragonal phase (fct), whereby the broadening of the diffraction peaks hinders the distinction between the observed fct phase and the Ll_0 structure of γ–TiAl [Fig. 4(a)]. In contrast, the different EFG clearly visible in the PAC data in Figs. 6(c) and 6(d) show that the local structure of the phase m-TiAl is different from that of γ–TiAl.

A DSC analysis of sample #A2 [Fig. 7, top panel] reveals four distinct exothermal peaks at 615, 710, 815, and 940 K, in contrast to only two observed at sample #A4 [Fig. 5]. Obviously, in the case of the shorter milling time, the behavior of the different Ti–Al phases is more complex than in the case of the sample milled for 13 h. Besides the DSC data of sample #A2, Fig. 7 (bottom panel) shows the fraction of ^{111}In atoms in the different crystalline environments observed by PAC during isochronal annealing. The comparison shows that the peak at 710 K can be assigned to the formation of the crystal structure characterized by $\overline{\nu_Q}$ = 38 MHz, the transition

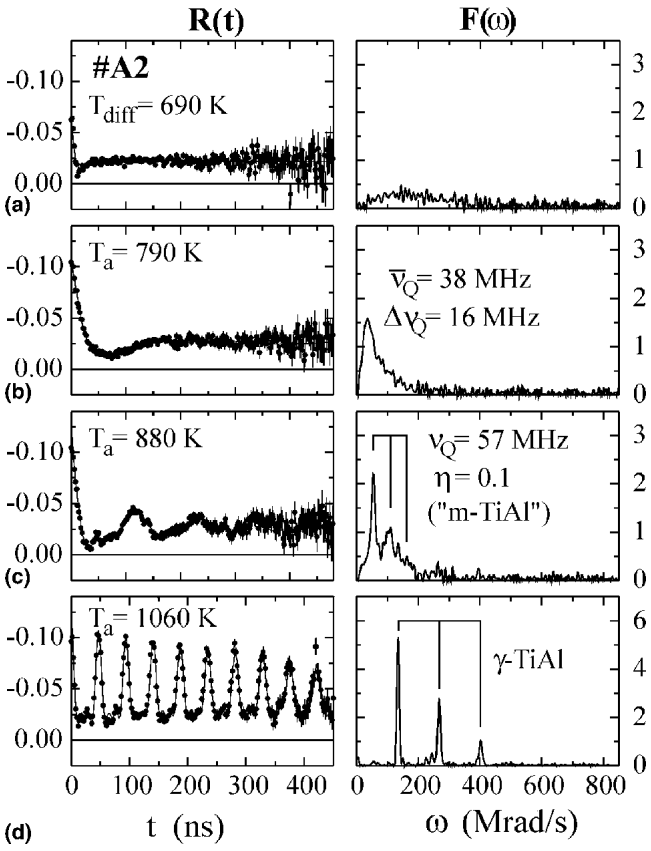

FIG. 6. PAC spectra of $Ti_{0.50}Al_{0.50}$ (#A2). The spectra were recorded after diffusion of ^{111}In at 690 K and after annealing at 790, 880, and 1060 K. An unknown crystalline structure is characterized by an EFG distribution of $\Delta\nu_Q$ = 16 MHz centered at $\overline{\nu_Q}$ = 38 MHz, the metastable phase m-TiAl by ν_Q = 57 MHz, η = 0.1, and γ–TiAl by ν_Q = 142 MHz, η = 0.

at 815 K to the formation of m-TiAl, and the peak at 940 K to the formation of γ–TiAl. A correlation of the peak at 615 K with a crystalline phase detected by PAC is not possible since the ^{111}In atoms were diffused into the sample at 690 K. Like the data in Fig. 6, the DSC and PAC data in Fig. 7 indicate that the EFG distribution, characterized by $\overline{\nu_Q}$ = 38 MHz and $\Delta\nu_Q$ = 16 MHz might represent a precursor state of m-TiAl. The corresponding crystal structure is still not identified and will not be further discussed in this paper.

The formation of the different phases as a function of the applied milling time was systematically investigated by PAC at $Ti_{0.50}Al_{0.50}$ samples annealed at T_a = 1060 K. Figure 8 shows the fraction of probe atoms incorporated in the phases γ–TiAl, m-TiAl, and Ti_2AlN. The equilibrium phase γ–TiAl and the impurity phase Ti_2AlN are formed in all samples with the exception of sample #A1 (t_{mill} = 2 h), for which the fraction of ^{111}In atoms in Ti_2AlN is obviously too small to be detected. The observation of a fraction of 30% of ^{111}In atoms incorporated in the metastable structure m-TiAl for a milling time of 2 h (#A1) and its absence for longer times indicates that at T_a = 1060 K after t_{mill} = 2 h the phase m-TiAl is thermally more stable than after t_{mill} = 4 h (#A2). For comparison, the PAC data of sample #A2 [Fig. 7, bottom panel] yield for m-TiAl a maximum fraction of about 50% at 880 K and almost zero at 1060 K. The fraction of Ti_2AlN increases monotonously with milling time from 0% (t_{mill} = 2 h) to 16% (t_{mill} = 23 h), whereas the fraction of γ–TiAl decreases from its maximum value of 67% (t_{mill} = 4 h) to 39% (t_{mill} = 23 h). The observed increase of the fraction of Ti_2AlN corresponds to an increasing level of N detected by chemical analysis (hot extraction combined with gas phase chromatography) yielding 3.2 at.% and 11.8 at.% after milling for 13 and 28 h, respectively. The total fraction of ^{111}In atoms in crystalline structures (Sum in Fig. 8) is almost constant up to a milling time of 13 h and decreases by about 15% for t_{mill} = 23 h. This decrease might be caused by probe atoms incorporated in a disordered structure, possibly caused by an increasing amount of contaminations.

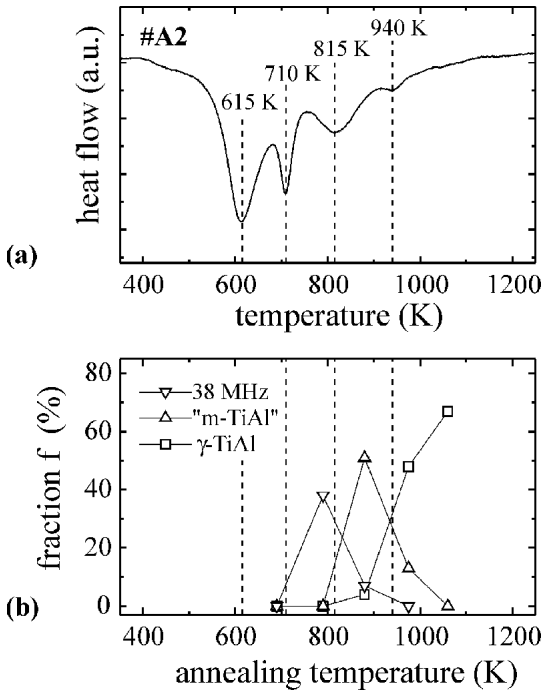

FIG. 7. For sample #A2, comparison of (a) DSC results and (b) the fraction of ^{111}In atoms observed by PAC in m-TiAl, γ–TiAl, and in the structure characterized by $\overline{\nu_Q}$ = 38 MHz.

B. $Ti_{0.75}Al_{0.25}$

Powders of the composition $Ti_{0.75}Al_{0.25}$ were mechanically alloyed and investigated as in the case of the $Ti_{0.50}Al_{0.50}$ alloys. The milling times were 16 and 52 h [Table I]. The evolution of the crystalline structure during heat treatment will be discussed in detail for sample #B1, milled for t_{mill} = 16 h.

After mechanical alloying of sample #B1, a solid solution with hcp structure was identified by XRD, which is in agreement with results reported in the literature.[12,13] The PAC spectrum recorded after diffusion of the ^{111}In probe atoms at 690 K for 16 h [Fig. 9(a)] reveals an EFG distribution similar to that observed in the $Ti_{0.50}Al_{0.50}$ samples. Annealing the sample at 880 K incorporates almost all ^{111}In probes into a local structure characterized by an EFG distribution $\Delta\nu_Q$ = 12 MHz, centered at $\overline{\nu_Q}$ = 32 MHz [Fig. 9(b)]. Increasing the annealing temperature to 1060 K slightly narrows this EFG distribution but does not significantly affect its position [Fig. 9(c)].

To identify the corresponding crystal structure, a second mechanically alloyed $Ti_{0.75}Al_{0.25}$ sample (supplied by R. Bormann, GKSS, Geesthacht, Germany) was investigated by PAC and XRD. The XRD spectrum recorded after annealing at 1060 K [Fig. 10] shows the hexagonal $D0_{19}$ structure of the intermetallic compound

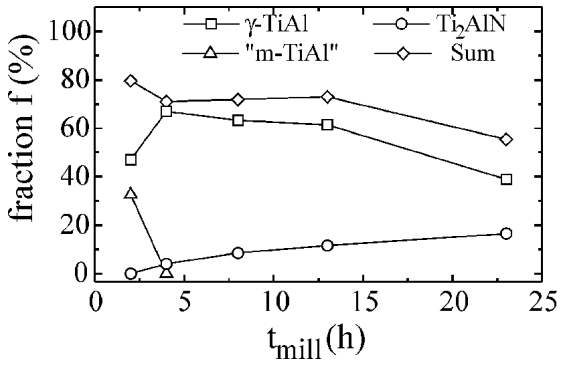

FIG. 8. For different milling times, the fraction of ^{111}In atoms incorporated in the phases m-TiAl, γ–TiAl and Ti_2AlN after annealing of the respective $Ti_{0.50}Al_{0.50}$ samples at 1060 K. The sum of all fractions is also plotted.

α_2–Ti_3Al [Fig. 3(b)]; the corresponding PAC spectrum was identical to that of sample #B1 shown in Fig. 9(c). Therefore, the observed EFG distribution about $\overline{\nu_Q} = 32$ MHz is assigned to the formation of the ordered crystal structure of α_2–Ti_3Al. The magnitude of the observed EFG characterizing this phase can be understood if the In probe atoms are on Al sites in this phase: in this case, the probe atom is surrounded by 12 Ti neighbors [Fig. 3(b)], so the short ranged EFG should be comparable to that of hexagonal α–Ti, for which PAC experiments yield $\nu_Q = 27.8$ MHz and $\eta = 0$.[16] Of particular importance is the measured distribution of EFG in the α_2–Ti_3Al structure of the present sample, which points to a superposition of slightly different, unresolved EFG. This occurrence can be caused by slightly different local configurations due to crystallites that are not perfectly ordered or by the presence of gaseous impurities (e.g., N, O, and H) incorporated in the neighborhood of the ^{111}In atoms.[17] These local perturbations of the α_2–Ti_3Al structure would not be expected on the basis of the XRD data in Fig. 10.

A DSC investigation of sample #B1 shows the coincidence of a single exothermal peak at 890 K [Fig. 11, top panel] with the annealing temperature that effects the occurrence of a fraction of more than 90% of ^{111}In atoms in α_2–Ti_3Al [Fig. 11, bottom panel]. Therefore, the DSC peak at 890 K is attributed to the transition from the disordered hcp solid solution prepared by ball milling to the ordered equilibrium phase α_2–Ti_3Al. At higher annealing temperatures, no additional transition is detectable neither by DSC nor by PAC [Fig. 9].

The influence of the milling time on the crystalline structure of $Ti_{0.75}Al_{0.25}$ powders was investigated by PAC for an annealing temperature of 1060 K. After a milling time of 16 h (#B1), all probe atoms were incorporated in the phase α_2–Ti_3Al [see Figs. 9(c) and 12(a)]. If the milling time is increased to 52 h (#B2), a pronounced formation of Ti_2AlN is observed [Fig. 12(b)]. The corresponding PAC data show that 55% of the ^{111}In atoms are incorporated in Ti_2AlN (Table II), and only 10% of the ^{111}In atoms in α_2–Ti_3Al. In contrast to the $Ti_{0.75}Al_{0.25}$ alloys, in the $Ti_{0.50}Al_{0.50}$ compounds the phase Ti_2AlN was already detectable for milling times of $t_{mill} = 4$ h [See Fig. 8].

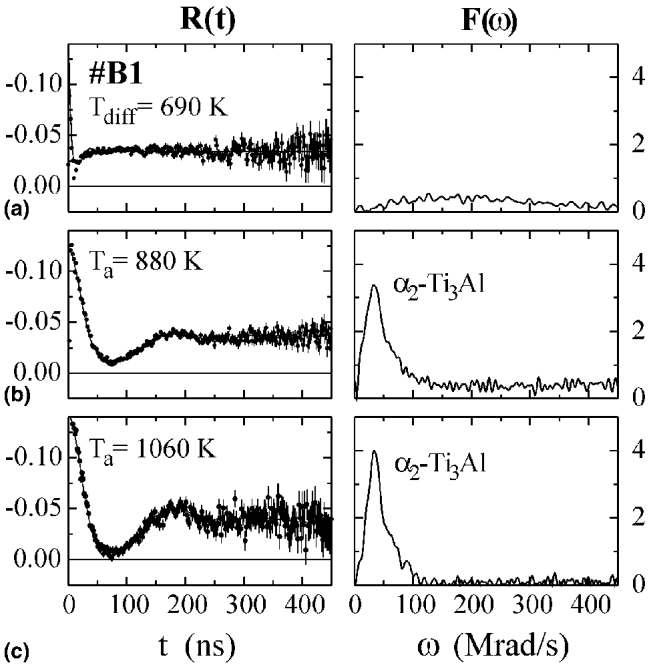

FIG. 9. PAC spectra of $Ti_{0.75}Al_{0.25}$ (#B1). The spectra were recorded after diffusion of ^{111}In at 690 K, and annealing at 880 and 1060 K.

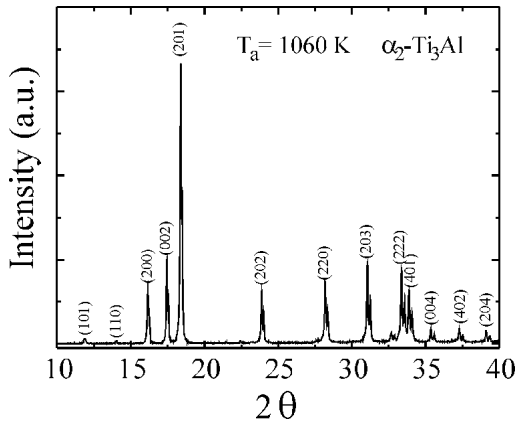

FIG. 10. XRD data of a mechanically alloyed $Ti_{0.75}Al_{0.25}$ sample (GKSS, Geesthacht) recorded after annealing at 1060 K.

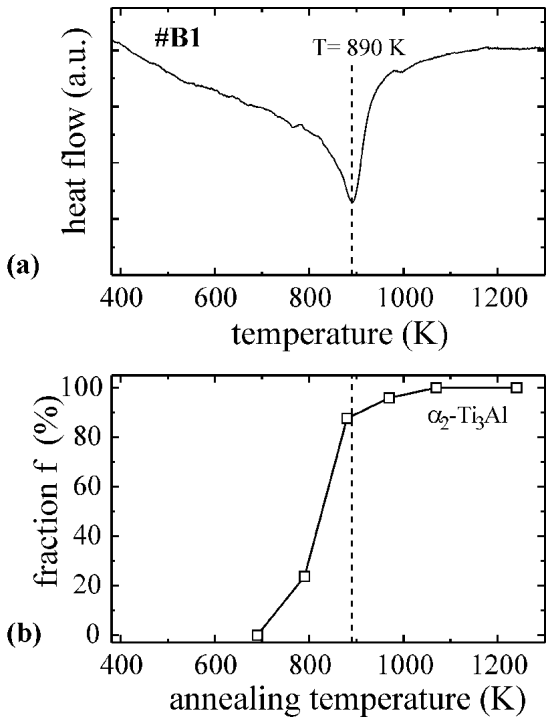

FIG. 11. For sample #B1, comparison of (a) DSC results and (b) the fraction of In atoms observed by PAC in α_2–Ti_3Al.

IV. DISCUSSION

The present PAC experiments reveal the formation of ordered intermetallic compounds upon annealing, having different noncubic crystal structures. The corresponding EFG measured at the site of the radioactive ^{111}In probe atoms are assigned to different intermetallic compounds of the Ti–Al system and are listed in Table II; the typical errors of the experimentally determined coupling constants υ_Q are on the order of 1 to 2 MHz. The experimental data show that each phase or local structure is characterized by its unique EFG in a reproducible way so that the EFG is used as a "fingerprint". As a group III element, the probe In should be incorporated on the Al site but based on atomic radii of the elements, the occupation of Ti sites is possible, too, as discussed elsewhere.[8] The actual lattice site of the ^{111}In probe is not of importance as long as the incorporation always happens on the identical lattice site; i.e., each phase or local structure has always its own fingerprint also under varying experimental conditions.

Since most experimental information was obtained for the $Ti_{0.50}Al_{0.50}$ compounds, the discussion will mainly focus on this material and will be extended to the $Ti_{0.75}Al_{0.25}$ compounds whenever possible. Tetragonal γ–TiAl, prepared by arc-melting, was investigated by Fan and Collins using PAC.[14] They showed that an EFG of $\upsilon_Q = 142$ MHz and $\eta = 0$ detected at the probe ^{111}In arises from the unperturbed lattice of the layered Ll_0 structure [Fig. 3(a)]. The identical EFG is observed in this work to occur after milling $Ti_{0.50}Al_{0.50}$ powder. Fan and Collins also reported the observation of a second EFG in γ–TiAl, characterized by $\upsilon_Q = 104.5$ MHz and $\eta = 0.46$ that, however, was revised later.[18]

The properties of mechanically alloyed Ti–Al compounds observed directly after ball milling vary significantly, as discussed in the literature.[19] The chosen milling conditions, such as type of ball mill, milling intensity, size of balls, and purity of argon atmosphere, strongly influence the results of the alloying process. It was shown by Oehring *et al.*[12] and by Park *et al.*[20] that $Ti_{0.50}Al_{0.50}$ powders become amorphous if the milling intensity is low. Additionally, the purity of the argon atmosphere influences the crystal structure arising during ball milling. In case of the compositions $Ti_{0.50}Al_{0.50}$ and $Ti_{0.75}Al_{0.25}$, high-purity conditions favor the formation of a hcp structure,[12] whereas under low purity conditions a face-centered-cubic (fcc) phase is obtained, which is assigned to TiN.[19,21,22] In the present experiments, contributions of amorphous phases were not detected by XRD. Following mechanical alloying, a hcp structure is observed by XRD for both $Ti_{0.50}Al_{0.50}$ and $Ti_{0.75}Al_{0.25}$, milled for 13 and 16 h, respectively. Since the solubility of Al in Ti is below 10% at room temperature, a supersaturated solid solution has been formed during ball milling in agreement with reports for the dissolution of Al in the hexagonal Ti lattice.[23] Using PAC, XRD, and DSC, the formation of ordered intermetallic compounds has been shown to occur after annealing the samples at high temperatures.

TABLE II. EFG observed in mechanically alloyed Ti–Al powders. In the case of an EFG distribution the mean value and the width $\Delta\upsilon_Q$ are given.

Structure	υ_Q (MHz)	η
γ–TiAl	142	0
Ti_2AlN	259	0
m-TiAl	57	0.1
α_2–Ti_3Al	$\overline{\upsilon_Q} = 32$	...
	$\Delta\upsilon_Q = 12$	

Following annealing at 1060 K, the equilibrium phases of the two compositions $Ti_{0.50}Al_{0.50}$ and $Ti_{0.75}Al_{0.25}$ are observable via the respective characteristic EFG of γ–TiAl and α_2–Ti_3Al, whereby in the latter case the EFG distribution indicates a slight lattice disorder. This heat treatment is comparable with the hot compaction of mechanically alloyed amorphous Ti–Al powders, described by various authors.[6,19,20] Hot compaction at temperatures between 1073 and 1473 K is reported to result in the formation of the intermetallic compounds α_2–Ti_3Al for the composition $Ti_{0.75}Al_{0.25}$, of γ–TiAl for $Ti_{0.50}Al_{0.50}$, and of τ–$TiAl_3$ for $Ti_{0.25}Al_{0.75}$,[19] which is consistent with the results presented here and in Ref. 8.[8]

Besides these phases, the present data show the formation of the impurity phase Ti_2AlN in $Ti_{0.50}Al_{0.50}$ and $Ti_{0.75}Al_{0.25}$. This phase was also reported in the case of $Ti_{0.25}Al_{0.75}$ samples studied by PAC using comparable experimental conditions.[8] The formation of Ti_2AlN after ball milling in a pure N_2 atmosphere and subsequent annealing was also observed at $Ti_{0.50}Al_{0.50}$ samples by Wang and co-workers[5] and by Chen and co-workers using a NH_3 atmosphere.[24] In these cases, the formation of γ–TiAl and Ti_2AlN was identified by XRD.

With regard to the transitions from the metastable structures into the respective equilibrium phases observed for Ti–Al compounds produced by mechanical alloying, the respective temperatures are determined by DSC investigations. The temperature of the transition to γ–TiAl determined in this work is systematically higher than corresponding literature values [See Table III]. This difference may be due to different parameters of the milling process or due to different concentrations of impurities. By comparing the present DSC data in Figs. 5 and 7 (top panels), it can be noted that the transition temperatures of γ–TiAl, determined for samples #A4 (1000 K) and #A2 (940 K), can be reproduced quite well. Nonetheless, the observed temperature difference of about 50 K seems to be significant and might be related to the different milling times used for these samples. Thus, the comparison of the present PAC and DSC experiments

on $Ti_{0.50}Al_{0.50}$ samples indicates that the DSC peaks at 845 and 1000 K correspond to the formation of Ti_2AlN and γ–TiAl, respectively. The corresponding temperatures in the literature are distributed over the range 870 to 1000 K. The exclusive formation of γ–TiAl at 870 K was observed by Istukaishi *et al.,*[19] whereas Senkov *et al.* determined a temperature of 995 K for this process.[25] After mechanical alloying in pure N_2 atmosphere, the simultaneous formation of both γ–TiAl and Ti_2AlN was observed to occur at 1000 K.[5] Furthermore, the data in Table III indicate that the transition temperatures do not seem to correlate with the initial crystalline phase, i.e., amorphous or solid solution, obtained after ball milling. On the contrary, as mentioned above, the PAC data suggest an influence of the milling time on the actual transition temperatures.

The structural evolution of the different phases depends on the degree of mechanical alloying. In the case of $Ti_{0.50}Al_{0.50}$, no elemental Ti and Al are observed by XRD after sufficiently long milling times, indicating that the alloying process is complete. After annealing at 1060 K, the equilibrium phases γ–TiAl and Ti_2AlN are observed by PAC, whereby the fraction of the impurity phase Ti_2AlN increases monotonously with increasing milling time [Fig. 8]. Since the chemical analysis also showed an increase of the N content of the samples with milling time, the N atoms obviously do not originate from contaminations of the elemental powders of the Ti and Al used as starting material but rather from residual N_2 in the Ar atmosphere present in the vials during ball milling.

The process of mechanical alloying is not complete in the case of shorter milling times, as in samples #A1 (t_{mill} = 2 h) and #A2 (t_{mill} = 4 h), and the XRD spectra still show the diffraction peaks of elemental Ti and Al. Consequently, the intermetallic phases observed at higher temperatures have to be formed by interdiffusion of both components during the subsequent thermal treatment. A new metastable structure (m-TiAl) is observed at T_a = 880 K, also with a fct crystal structure like γ–TiAl as determined by XRD. In contrast, the PAC data show a well-defined EFG, which is characteristic for a locally ordered structure and is different from the EFG of γ–TiAl. Thus, the phase m-TiAl is obviously chemically ordered, but the atomic arrangement of Ti and Al atoms is different from that in γ–TiAl. For this new phase, which was observed in different samples, the formation conditions, like milling time and annealing temperature, as well as the thermal stability and transition temperature [See Figs. 7 and 8] are determined. Due to the short milling time, the fraction of the impurity phase Ti_2AlN remained at a low level in these samples. It should be noted that a metastable Ti–Al phase was also observed in mechanically alloyed $Ti_{0.25}Al_{0.75}$ samples.[8] In this case, annealing at 690 K caused the formation of $TiAl_3$ with a metastable $D0_{23}$ crystal structure, which transformed into the $D0_{22}$ equilibrium structure following heat treatment at 1020 K.

In the $Ti_{0.75}Al_{0.25}$ alloys, besides τ–$TiAl_3$, the impurity phase Ti_2AlN is not observable after annealing at 1060 K if the milling time is 16 h (sample #B1), whereas in sample #B2, which was milled for 52 h, most of the ^{111}In probe atoms are incorporated into Ti_2AlN [Fig. 12]. The absence of Ti_2AlN after 16 h is confirmed by the DSC data, which show only a single peak. After a similar milling time of 13 h, in $Ti_{0.50}Al_{0.50}$ alloys, this phase was already clearly visible under comparable preparation conditions (sample #A4 in Fig. 2). In the case of sample #B1, the N impurity atoms obviously do not form an ordered compound in the $Ti_{0.75}Al_{0.25}$ sample in contrast to the $Ti_{0.50}Al_{0.50}$ samples. Rather, the N impurities seem to be dissolved in the α_2–Ti_3Al lattice, which

TABLE III. Thermal stabilities of crystalline phases prepared by mechanical alloying and their transformation into intermetallic compounds. The transition temperatures were determined by DSC.

Composition	Initial structure	Transition temperature (K)	Intermetallic compound	Reference
$Ti_{0.50}Al_{0.50}$	hcp	1000, 845	γ–TiAl, Ti_2AlN	this work
	hcp	850	...[a]	12
	amorphous	870	γ–TiAl	19
	amorphous	1000	γ–TiAl, Ti_2AlN	5
$Ti_{0.50}Al_{0.47}Cr_{0.03}$	amorphous	900, 995[b]	hcp, γ–TiAl	25
$Ti_{0.75}Al_{0.25}$	hcp	890	α_2–Ti_3Al	this work
	hcp	730	...[a]	12
	amorphous + hcp + fcc	850	α_2–Ti_3Al	19

[a]The corresponding intermetallic compounds are not specified.

[b]A twofold transformation from an amorphous phase to hcp and from hcp to γ–TiAl is observed.

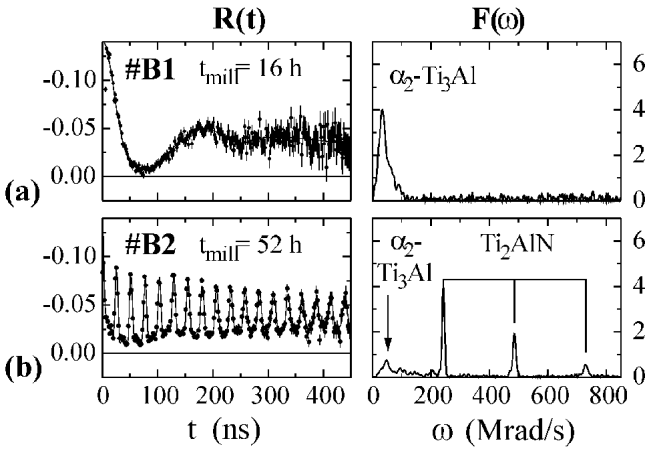

FIG. 12. For two different milling times, PAC spectra of $Ti_{0.75}Al_{0.25}$ samples (#B1 and #B2) measured after annealing at 1060 K.

would explain the absence of the Ti_2AlN phase and, at the same time, the EFG distribution observed for α_2–Ti_3Al [See Table II]. The occurrence of the EFG distribution characterized by $\Delta\nu_Q = 12$ MHz and $\overline{\nu_Q} = 32$ MHz is in sharp contrast to the unique EFG, observed in case of γ–TiAl and τ–$TiAl_3$.[8] At the same time, the EFG distribution shows the presence of local disorder, which is not easily recognizable in the corresponding XRD data [See Fig. 10].

V. SUMMARY

PAC spectroscopy complemented by XRD and DSC was applied to investigate the formation of intermetallic compounds in mechanically alloyed Ti–Al samples. The measured EFGs show the formation of γ–TiAl, α_2–Ti_3Al, Ti_2AlN, and of a new metastable fct structure m-TiAl. The experimental results obtained by employing the PAC technique for the study of mechanically alloyed samples show the following:

(1) Since PAC is sensitive to the local order on an atomic scale it complements other techniques such as XRD. As a consequence, information was obtained about a new metastable phase m-TiAl and about the slight structural or chemical disorder in the case of the formation of α_2–Ti_3Al.

(2) PAC can be combined with other analytical techniques under identical sample conditions. In the present study, PAC was combined with XRD and DSC measurements using samples from the identical milling process so that the results obtained by the three different techniques were directly comparable.

(3) The short-range EFG warrants a high sensitivity for the detection of impurities, crystal defects, and small grains. As was shown in the case of the investigation of $TiAl_3$ compounds, the fraction of Ti_2AlN was too small to be visible to XRD but was still detectable by PAC.[8] Similarly, the investigation of the local structures in grain boundaries might become possible as has been documented by first results in nanocrystalline Ni prepared by pulsed electrodeposition.[26]

In conclusion, the present work performed in combination with XRD and DSC represents a first systematic investigation of the formation of different phases in mechanically alloyed Ti–Al compounds on an atomic scale and thereby has contributed to a more complete picture of the evolution of different phases during ball milling.

ACKNOWLEDGMENTS

The authors would like to thank Dr. C.E. Krill and Dipl.Ing. J. Schmauch (Lehrstuhl Prof. Dr. R. Birringer) for performing the XRD and DSC measurements. We thank Prof. R. Bormann, Prof. R. Wagner (GKSS Geesthacht, Germany), and their co-workers for the supply of various Ti–Al samples. Financial support by the Deutsche Forschungsgemeinschaft (SFB 277) is gratefully acknowledged.

REFERENCES

1. H.A. Lipsitt, in *High-Temperature Ordered Intermetallic Alloys,* edited by C.C. Koch, C.T. Liu, and N.S. Stoloff, (Mat. Res. Soc. Symp. Proc. **39,** Pittsburgh, PA, 1985), p. 351.
2. H. Mabuchi, H. Tsuda, Y. Nakayama, and E. Sukedai, J. Mater. Res. **7,** 894 (1992).
3. C.C. Koch, Mater. Sci. Forum **88–90,** 243 (1992).
4. R.D. Schelleng, J. Metals **41**(1), 32 (1989).
5. K.Y. Wang, J.G. Wang, and G.L. Chen, J. Mater. Res. **10,** 1247 (1995).
6. T. Suzuki, T. Ino, and M. Nagumo, Mater. Sci. Forum **88–90,** 639 (1992).
7. *Hyperfine Interactions in Nanocrystalline Materials,* edited by G.S. Collins (Hyp. Int. **130,** Dordrecht, The Netherlands, 2000).
8. St. Lauer, Z. Guan, H. Wolf, and Th. Wichert, Mater. Sci. Forum **269–272,** 485 (1998).
9. G. Schatz, A. Weidinger, *Nuclear Condensed Matter Physics* (Wiley, Chichester, England, 1995), p. 63.
10. Th. Wichert and E. Recknagel, in *Microscopic Methods in Metals,* edited by U. Gonser (Topics in Current Physics **40,** Berlin, Germany, 1986), p. 317.
11. G.K. Williamson and W.H. Hall, Acta Metall. **1,** 22 (1953).
12. M. Oehring, T. Klassen, and R. Bormann, J. Mater. Res. **8,** 2819 (1993).
13. G. Walkowiak, T. Sell, and H. Mehrer, Z. Metallkd. **85,** 332 (1994).
14. J. Fan and G.S. Collins, Hyp. Int. **79,** 745 (1993).
15. St. Lauer, H. Wolf, H. Ehrhardt, H.G. Zimmer, and Th. Wichert, Hyp. Int. **C1,** 262 (1996).
16. E.N. Kaufmann, P. Raghavan, R.S. Raghavan, K. Krien, and R.A. Naumann, Phys. Status Sol. **63,** 719 (1974).
17. H. Foettinger, D. Forkel, H. Plank, and W. Witthuhn, Hyp. Int. **35,** 765 (1987).
18. G.S. Collins, (private communication).
19. T. Itsukaichi, K. Masuyama, M. Umemoto, I. Okane, and J.G. Cabañas-Moreno, J. Mater. Res. **8,** 1817 (1993).
20. Y.H. Park, H. Hashimoto, and R. Watanabe, Mater. Sci. Forum **88–90,** 59 (1992).
21. C. Suryanarayana, Intermetallics **3,** 153 (1995).
22. W. Guo, S. Martelli, F. Padella, M. Magini, N. Burgio, E. Paradiso, and U. Franzoni, Mater. Sci. Forum **88–90,** 139 (1992).
23. T. Klassen, M. Oehring, and R. Bormann, J. Mater. Res. **9,** 47 (1994).
24. Y. Chen, A. Calka, J.S. Williams, and B.W. Ninham, Mater. Sci. Eng. **A187,** 51 (1994).
25. O.N. Senkov, N. Srisukhumbowornchai, M.L. Övecoglu, and F.H. Froes, J. Mater. Res. **13,** 3399 (1998).
26. H. Wolf, Z. Guan, X. Li, and Th. Wichert, Hyp. Int. (2002, in press).